


# Fog collection on a conical copper wire: effect of fog flow velocity and surface morphology

Haiting Xing, Jiang Cheng , Cailong Zhou, Yanfen Zheng, Gang Wang, Xiufang Wen, Pihui Pi, Shouping Xu

School of Chemistry and Chemical Engineering, South China University of Technology, Guangzhou 510640, People's Republic of China

✉ E-mail: cejcheng@scut.edu.cn

Published in Micro & Nano Letters; Received on 6th December 2017; Revised on 27th March 2018; Accepted on 12th April 2018

The conical copper wires (CCWs) were subjected to alkali assistant oxidation or electrochemical deposition to form superhydrophilic wettability of  $\sim 4^\circ$  with needle-like or leaf-like morphology, respectively. The superhydrophobic CCWs with water contact angles of  $\sim 156^\circ$  were further constructed by modification with 1-dodecanethiol. The CCWs were used to study the effect of fog flow velocity and surface morphology on fog collection. With the fog flow velocity increased, the dominant factor for fog collection changed from fog capture to droplet motion. The surfaces with needle-like morphology displayed better fog capture ability while the surfaces with leaf-like morphology were more prone to driving droplet motion.

**1. Introduction:** Lots of attentions were paid to fog collection in recent years due to the growing fresh water crisis arisen from expansion of arid region and pollution of water resource [1]. Quite a few studies concentrated on desert biology like beetles [2, 3], cacti [4, 5], *Cotula fallax* plants [6] and *Stipagrostis subulicola* grass [7, 8], which can collect rare water from fog. As the most common biology among them, cacti were studied from many aspects. The reported studies, however, mostly based on the abundant fog flow rather than the ordinary circumstance. Early in 1991, Schemenauer and Cereceda [9] reported that the fog-laden wind speed was one of the factors that influenced fog collection efficiency. Peng *et al.* [10] concluded that the wind played an important role in fog collection by a magnetically induced fog collection experiment. Therefore, it is necessary to study the influence of fog flow velocity on fog collection in detail.

On the other hand, though the same wettability can be prepared by different methods, the surface nanostructures are usually not identical. However, the detailed influence of different surface nanostructures on fog collection, especially on fog capture and droplet motion, still remains uncertainty. To the best of our knowledge, few references concerned this section in fog collection. Some of the researchers, such as Azad *et al.*, found that the microgroove surface showed higher efficiency of fog collection than smooth one by two to three times, suggesting that the surface nanostructure mattered on fog collection indeed [11].

Therefore, in this work we prepared the conical copper wires (CCWs), with needle-like and leaf-like surface morphologies, to investigate their fog collection ability especially the performance of fog capture and droplet motion under various fog flow velocities.

**2. Experimental:** The pre-cleaned copper wire with 0.4 mm of diameter and 20 mm of length was corroded by electrochemical oxidation. The anode, cathode and electrolyte were pre-cleaned copper wire, graphite and  $2 \text{ mol l}^{-1}$  NaOH solution, respectively. With the electrolyte extracted slowly by a pump, the anode was corroded in different degree along the latitude and became the sample of CCW (apex angle  $2\alpha \approx 4^\circ$ ). Superhydrophilic surfaces on the CCWs were prepared by alkali assistant oxidation (AAO) and electrochemical deposition (ECD) (named, respectively, as AAO-CCW and ECD-CCW below). In AAO method [12, 13], the CCW was immersed into a mixture of  $0.75 \text{ mol l}^{-1}$  NaOH and  $0.0375 \text{ mol l}^{-1}$   $(\text{NH}_4)_2\text{S}_2\text{O}_8$  for 9 min. In ECD method,

the CCW (cathode) and graphite (anode) were electrolysed in a mixture of  $0.005 \text{ mol l}^{-1}$   $\text{CuSO}_4$  and  $0.1 \text{ mol l}^{-1}$   $\text{H}_2\text{SO}_4$  for 4.5 min. Superhydrophobic CCWs were fabricated by modifying the superhydrophilic ones with  $0.001 \text{ mol l}^{-1}$  of 1-dodecanethiol ethanol solution.

The crystallographic structures of CCW surface were determined by X-ray diffraction (XRD, Bruker D8 Advance). The surface morphology was observed by a scanning electron microscope (SEM, Zeiss Merlin). Water contact angles (WCAs) were measured by a contact angle analyser (Shanghai Zhonghui Powereach JC2000D1A) with  $3 \mu\text{l}$  of individual water droplet.

During fog collection, a CCW, whose apex was up-tilted at  $45^\circ$ , captured the fog generated by a humidifier fixed on top of the CCW 40 mm away. In fog capture, the CCW and humidifier were placed as the fog collection experiment, but as soon as the fog gathered into droplet, the droplet would be taken off quickly before it moved. In droplet motion, a droplet of  $1 \mu\text{l}$  was added on the apex point of a horizontally placed CCW (17 mm efficient length), the whole moving process was shot by a high-speed industrial camera (Baumer HXC20) at 337 frames per second.

**3. Results and discussion:** Figs. 1a and b show the SEM images of the surfaces of AAO-CCW and ECD-CCW with morphologies of needle-like and leaf-like, respectively, and both structures fall into the nanoscale. From XRD patterns (Fig. 1c) all the peaks marked with black dot and hollow triangle could be indexed to orthorhombic-phase  $\text{Cu}(\text{OH})_2$  (JCPDS Card No. 72-0140) and orthorhombic-phase Cu (JCPDS Card No. 85-1326), respectively. No other peaks were found, indicating only  $\text{Cu}(\text{OH})_2$  and Cu grew on AAO-CCW and ECD-CCW surfaces, respectively.

The WCAs on the surfaces of as-prepared AAO-CCW and ECD-CCW could reach  $4.6^\circ$  (Fig. 1d1) and  $4.3^\circ$  (Fig. 1d3), respectively. Through an ECD method, the deposited copper was rougher than the original copper substrate, making the surface more hydrophilic according to Wenzel model [14], similar as the previous work by Zhang *et al.* [15]. After modification with 1-dodecanethiol, the resultant CCWs showed good superhydrophobicity with the WCAs of  $155.8^\circ$  (AAO-CCW, Fig. 1d2) and  $156.0^\circ$  (ECD-CCW, Fig. 1d4), respectively, due to the combination of its low surface energy and considerable roughness provided by the surface structures.

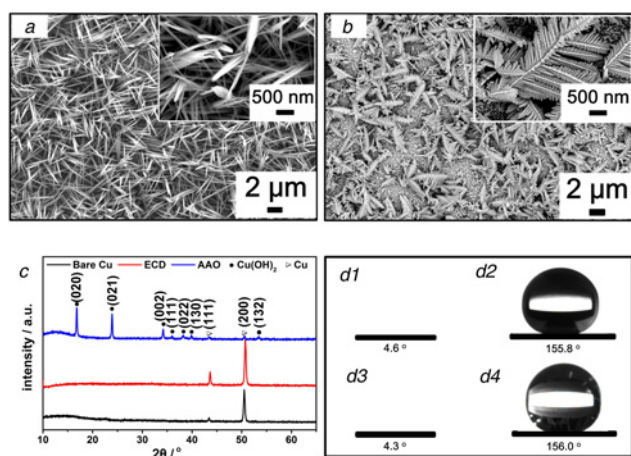


**Fig. 1** SEM images (the insets are the images with larger magnification), XRD patterns and WCAs of the surfaces  
a SEM images of the surfaces of AAO-CCW  
b SEM images of the surfaces of ECD-CCW  
c XRD patterns of the pristine CCW (black), AAO-CCW (blue) and ECD-CCW (red)  
d1 WCAs of superhydrophilic AAO-CCWs  
d2 WCAs of superhydrophobic AAO-CCWs  
d3 WCAs of superhydrophilic ECD-CCWs  
d4 WCAs of superhydrophobic ECD-CCWs

Fig. 2a displays the fog collection under various fog flow velocities on different wetting CCWs. The droplets on the superhydrophilic surfaces (both AAO and ECD) are oval and could slip away easily while those on the superhydrophobic surfaces (both AAO and ECD) are spherical and stick to their original position, similar to the phenomenon reported in [16]. When the fog flow velocity was  $<50 \text{ cm s}^{-1}$ , the superhydrophobic surfaces collected more water than superhydrophilic ones did. However, the fog collection ability of the CCWs reversed when the fog flow velocity was above  $50 \text{ cm s}^{-1}$ , indicating the fog flow velocity plays an important role on fog collection and CCWs with different wetting perform differently.

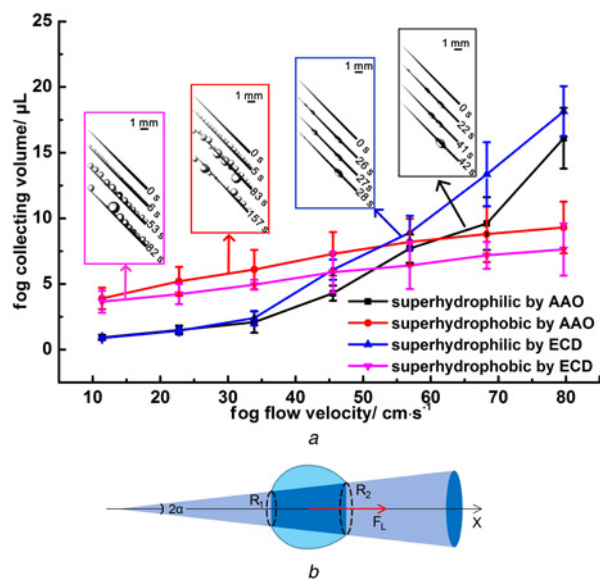


**Fig. 2** Fog collecting volume and illustration of droplet on the CCW  
a Fog collecting volume versus fog flow velocity on the CCWs in 30 min. The insets are photographs of the fog collection under  $59.6 \text{ cm s}^{-1}$  of fog flow velocity  
b Illustration of droplet on the CCW

Fig. 2b is the illustration of a droplet on a CCW. The procedure of fog collection on CCW could be divided into two steps including fog capture and droplet motion. Apparently, the superhydrophobic surface has relatively smaller water-surface contact area, making more water droplet stand and gather together on the CCW. Meanwhile, smaller water-surface contact area could decrease the re-evaporation, thus preventing droplet converting back to fog. So the superhydrophobic surface is beneficial to the fog capture. On the other hand, superhydrophilic surface possesses larger water-surface contact area, leading to a more difference between the tip radius ( $R_1$ ) and root radius ( $R_2$ ), further causing a raise of the driving Laplace force ( $F_L$ ). Furthermore, water on superhydrophilic surface would form a lubrication film, reducing the resistance in the process of droplet motion. Therefore, the superhydrophilic surface is helpful to the droplet motion [16–18]. In view of the superhydrophobic and superhydrophilic surfaces collected more fog under relatively smaller and larger fog flow velocity, respectively, it can be concluded that with the fog flow velocity increased, the dominant factor of fog collection changed from fog capture to droplet motion.

Based on the differences in fog collection between the two kinds of morphologies shown in Fig. 2a, we further investigated the effect of surface morphology on the fog capture and drop motion velocity. As shown in Fig. 3, the fog capture velocity of the superhydrophobic CCWs (both AAO and ECD) increased along with the increasing of fog flow velocity, and the fog capture ability of the surface with needle-like morphology made by AAO was always better than that of the surface with leaf-like morphology made by ECD under various fog flow velocities. The needle-like nanoarrays are bumpy but the leaf-like nanoarrays are relatively flat, leading to the different amount of surface exposed to the surrounding fog. The bumpy needle-like nanoarrays made better use of surface area than flat leaf-like nanoarrays. More available surface may contribute to better fog capture, hence the surface with needle-like morphology captured more fog than the leaf-like one did.

As demonstrated in Figs. 4a3 and b3, the droplet motion on the surface with leaf-like morphology was quicker than that on the surface with needle-like morphology by 6.2%. As described before, the lubrication effect could be in favour of the drop motion. The needle-like nanostructure might block the droplet into the interspace, holding it to stick to the primary position (Figs. 4a1 and a2) whereas the leaf-like nanostructure was easier to let the water micro-droplets slip away thanks to the relatively flat surface, resulting in fast droplet motion (Figs. 4b1 and b2). Consequently, the droplet motion velocity of the surface with leaf-like morphology was faster than the needle-like one did.

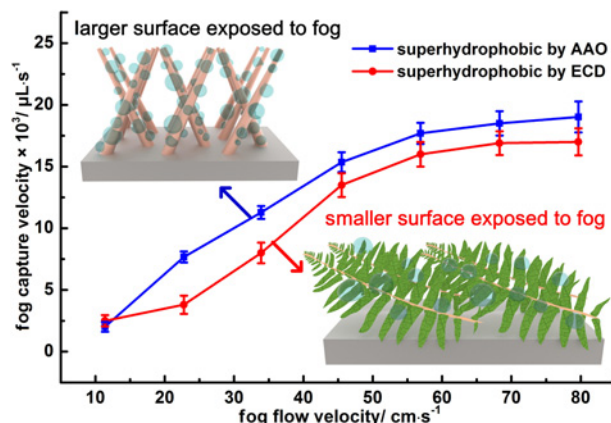


**Fig. 3** Fog capture velocity of the superhydrophobic CCWs under different fog flow velocities. The insets are the scheme of fog capture on surfaces with needle-like and leaf-like morphology, respectively

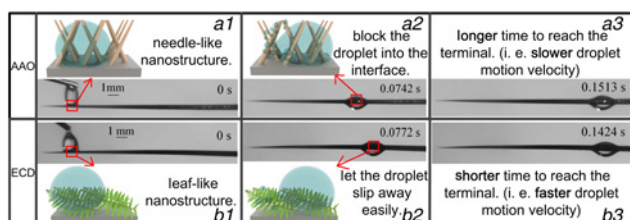


**Fig. 4** Photographs of droplet motion, the insets are illustration of the surfaces

- a1 Droplet motion on superhydrophilic AAO-CCW at 0 s  
a2 Droplet motion on superhydrophilic AAO-CCW at 0.0742 s  
a3 Droplet motion on superhydrophilic AAO-CCW at 0.1513 s  
b1 Droplet motion on superhydrophilic ECD-CCW at 0 s  
b2 Droplet motion on superhydrophilic ECD-CCW at 0.0772 s  
b3 Droplet motion on superhydrophilic ECD-CCW at 0.1424 s

**4. Conclusion:** In summary, when fog flow velocity is  $< 50 \text{ cm s}^{-1}$ , superhydrophobic surface with needle-like morphology obtains faster fog collection velocity due to their stronger abilities of fog capture. Whereas, when fog flow velocity is more than  $50 \text{ cm s}^{-1}$ , superhydrophilic surface with leaf-like morphology displays faster fog collection velocity because of better droplet motion performance. Generally, during the fog collection process, the dominant factor changes from fog capture velocity to droplet motion velocity with the fog flow velocity increased. Meanwhile, the surface with needle-like morphology captures fog faster while the surface with leaf-like morphology moves droplet more rapidly. Thus, to realise the best fog collection efficiency, superhydrophobic CCW with needle-like nanostructure (or other nanostructure with more surface exposed to fog) is suggested when fog flow velocity is smaller than  $50 \text{ cm s}^{-1}$  and superhydrophilic CCW with leaf-like nanostructure (or other relatively ‘flat’ nanostructure) should be applied when fog flow velocity is  $> 50 \text{ cm s}^{-1}$ .

**5. Acknowledgment:** This work was supported by the National Natural Science Foundation of China (grant no. 21776094).

## 6 References

- [1] Zhang B.Q., Long B., Wu Z.Y.: ‘An evaluation of the performance and the contribution of different modified water demand estimates

- in drought modeling over water-stressed regions’, *Land Degrad. Dev.*, 2017, **28**, pp. 1134–1151  
[2] Parker A.R., Lawrence C.R.: ‘Water capture by a desert beetle’, *Nature*, 2001, **414**, pp. 33–34  
[3] Nørgaard T., Dacke M.: ‘Fog-basking behaviour and water collection efficiency in Namib Desert darkling beetles’, *Front. Zool.*, 2010, **7**, p. 23  
[4] Ju J., Bai H., Zheng Y.M., *ET AL.*: ‘A multi-structural and multi-functional integrated fog collection system in cactus’, *Nat. Commun.*, 2012, **3**, pp. 2253–2258  
[5] Heng X., Xiang M., Lu Z., *ET AL.*: ‘Branched ZnO wire structures for water collection inspired by cacti’, *Appl. Mater. Inter.*, 2014, **6**, pp. 8032–8041  
[6] Andrews H., Eccles E., Schofield W., *ET AL.*: ‘Three-dimensional hierarchical structures for fog harvesting’, *Langmuir*, 2011, **27**, pp. 3798–3802  
[7] Ebner M., Miranda T., Roth-Nebelsick A.: ‘Efficient fog harvesting by *Stipagrostis sabulicola* (namib dune bushman grass)’, *J. Arid Environ.*, 2011, **75**, pp. 524–531  
[8] Nørgaard T., Ebner M., Dacke M.: ‘Animal or plant: which is the better fog water collector?’, *Plos One*, 2012, **7**, p. e34603  
[9] Schemenauer R.S., Cereceda P.: ‘Fog-water collection in arid coastal locations’, *Ambio*, 1991, **207**, pp. 303–308  
[10] Peng Y., He Y.X., Yang S., *ET AL.*: ‘Magnetically induced fog harvesting via flexible conical arrays’, *Adv. Funct. Mater.*, 2015, **25**, pp. 5967–5971  
[11] Azad M.A.K., Ellerbrok D., Barthlott W., *ET AL.*: ‘Fog collecting biomimetic surfaces: influence of microstructure and wettability’, *Bioinspir. Biomim.*, 2015, **10**, p. 016004  
[12] Zhou C.L., Li H.J., Lin J., *ET AL.*: ‘Matchstick-like  $\text{Cu}_2\text{S}/\text{Cu}_x\text{O}$  nanowire film: transition of superhydrophilicity to superhydrophobicity’, *J. Phys. Chem. C*, 2017, **121**, pp. 19716–19726  
[13] Zhou C.L., Zhao A., Cheng J., *ET AL.*: ‘ $\text{Cu}_2\text{O}$  nanoribbons on copper mesh with underwater superoleophobicity for oil/ water separation’, *Mater. Lett.*, 2016, **185**, pp. 403–406  
[14] Wenzel R.N.: ‘Resistance of solid surfaces to wetting by water’, *Ind. Eng. Chem.*, 1936, **28**, pp. 988–994  
[15] Zhang E., Cheng Z.J., Lv T., *ET AL.*: ‘Anti-corrosive hierarchical structured copper mesh film with superhydrophilicity and underwater low adhesive superoleophobicity for highly efficient oil-water separation’, *J. Mater. Chem. A*, 2015, **3**, pp. 13411–13417  
[16] Azad M. A. K., Barthlott W., Koch K.: ‘Hierarchical surface architecture of plants as an inspiration for biomimetic fog collectors’, *Langmuir*, 2015, **31**, (48), pp. 13172–13179  
[17] Lorenceau E., Quéré D.: ‘Drops on a conical wire’, *J. Fluid Mech.*, 2004, **510**, pp. 29–45  
[18] Ju J., Xiao K., Yao X.: ‘Bioinspired conical copper wire with gradient wettability for continuous and efficient fog collection’, *Adv. Mater.*, 2013, **25**, (41), pp. 5937–5942